Kuwait J.Sci., Vol.49, No.(2),April.2022,pp(1-15)

Implementing electrical resistivity tomography to delineate soil contamination zone, Southern Baqubah City, Iraq

Munther D. Al-Awsi[1], Zaidoon T. Abdulrazzaq[2,*]

[1] *Dept. of Petroleum Geology and Mineral, Diyala University, Iraq*
[2] *Directorate of Space and Communications, Ministry of Science and Technology, Iraq*
[*] *Corresponding author: zaidoon.taha@live.com*

Abstract

An electrical resistivity tomography survey was carried out on the Diyala University campus, southern Baqubaa city, Iraq. The main aim of this study is to evaluate the efficiency of electrical resistivity tomography to detect the buried sewage system as well as to assess its environmental impact on the surrounding soil. Six parallel resistivity profiles were carried out in a perpendicular direction to the axis of the sewage system. Two-and three-dimensional geoelectrical models were constructed to determine the distribution of resistivity and its relation with both buried structures and contaminated zones. The results showed an intermediate relative resistivity zone (6-10 Ω.m) and several rounded very low resistivity zones (< 1 Ω.m), identifying the underground sewage system and contaminated soil, respectively. Based on variations in resistivity values, six holes (h1, h2, h3, h4, h5, and h6) were drilled. A total of six soil samples at 1.5m depth (1 sample per hole) were collected for heavy metals concentrations analysis. The results of the chemical analysis showed a higher concentration of heavy metals near the septic system than that in the area away from it. Much lower resistivity zones (<1 Ω.m) and the higher concentration of heavy metals observed near the septic system indicate the impact of contamination by migration from the septic tank into the nearby soil. The results of this study confirm the efficiency of electrical resistivity tomography for detecting a buried object and mapping contaminated zone for engineering and environmental applications.

Keywords: Chemical analysis; contamination; electrical resistivity tomography; environmental application; heavy metals.

1. Introduction

Contamination of soil by heavy metals is a widespread environmental problem and has become a severe challenge for life because of its effects on human health (Kabata-Pendias, 2010). Heavy metals in soils are generated naturally or from anthropogenic activities in developed countries (Wang *et al*., 2019). The waste and sewage management sectors are one of the main contributors to anthropogenic contamination (Chik *et al*., 2014; Hamed *et al*., 2017). The existence of contaminants in the environment needs a detailed description of the extent and nature of contamination for active remediation. Traditional environmental monitoring has concentrated on

point sampling, which usually includes intrusive methods such as drilling (Aizebeokhai, 2009). This method is expensive, destructive in nature, consumes much time, and gives information only on effects at the sampling site (Granato & Smith, 1999). Non-invasive methods, such as geophysical techniques, are more effective alternative methods that have been applied in environmental monitoring applications (Abdulrazzaq *et al*., 2020). They offer a rapid and cost-effective means of imaging the subsurface structures with logical resolution (Metwaly & AlFouzan, 2013; Abed *et al.,* 2020). The existence of contaminants in soils and water alters their physical properties. The amount of alteration depends on the concentration and nature of contaminants in addition to the period of contamination (Aizebeokhai, 2009). Therefore, many environmental problems can be resolved by geophysical methods (Rao *et al*., 2014). Electrical resistivity tomography is one of the most effective geophysical methods used to image the subsurface using differences in measured electrical resistivity at the surface (Dahlin, 2001). For this reason, ERT is the best-known geophysical technique in hydrogeological settings for groundwater description and monitoring (Rizzo & Valeria, 2019). Recently, the resistivity method has been widely used around the world to monitor and assess possible contamination of groundwater and soils (Thabit & Khalid, 2016; Gemail *et al*., 2017; Giang *et al*., 2018; Nasir *et al*., 2021). In environmental studies, monitoring of contaminated water and soil is usually carried out by integrating the results of chemical analysis and resistivity measurements (Amidu & Olayinka, 2006; Hamzah *et al*., 2014; Olaseeni *et al*., 2018; Aziz *et al*., 2019). Due to the conductive nature of the most contaminant, the resistivity values appear as a low resistivity anomaly zone. In other word, the resistivity values of contaminated soil decrease with an increase of heavy metal concentration (Liu *et al*., 2016; Wang *et al*., 2019). In the current study, and according to available information, a buried sewage system receives sewage from the building's sewer daily. Therefore, different degrees of environmental impact have been foreseen. This study aimed to investigate the reliability of the ERT technique for detecting buried sewage systems and to assess (if any) the environmental influence of the septic system on the surrounding soil. This involved geo-environmental studies, using electrical resistivity tomography and chemical analysis across a septic tank within the University of Diyala campus, northeastern Iraq. Chemical analysis was used to identify the concentration of heavy metals in six soil samples taken at pre-established points (at 1.5 m depth) within the investigated area. The current study represents the first study using the ERT technique to evaluate contamination of soils in Baqubah city.

2. Site Description

The study area is located near the college of science at the University of Diyala campus, southern Baqubah city, 60 km northeast Baghdad governorate (Figure 1). The study area is flat, and the approximate elevation is about 35 m above sea level. Geologically the site lies within the Mesopotamian plain and is covered by thick fluvial sediment (Jassim & Goof, 2006). To explore the subsoil conditions of the proposed sites of new buildings at Diyala University, eighty-five (85) boreholes were drilled at different depths by Al-Ebdaa Company for soil investigation (2015).

According to these boreholes, the soil profile is the same in all the excavated points and consists of three main layers (Figure 2). The uppermost layer consists of light to dark low plasticity clay. The middle layer consists of dark gray silty sand. The bottom layer consists of dark gray, poorly graded sand extending to the end of poring (Al-Ebdaa Company, 2015). The investigated site was selected because it consists of known subsurface features, such as covered monsoon drain, underground concrete sewage system, and manhole columns. Depending on the location of the manhole, the direction and location of the sewage system can be anticipated. This system receives sewage from a building sewer daily. Therefore, the current study was conducted to detect the capability of resistivity imaging technique for detecting buried sewage systems and to assess (if there) its environmental impact on the surrounding soil.

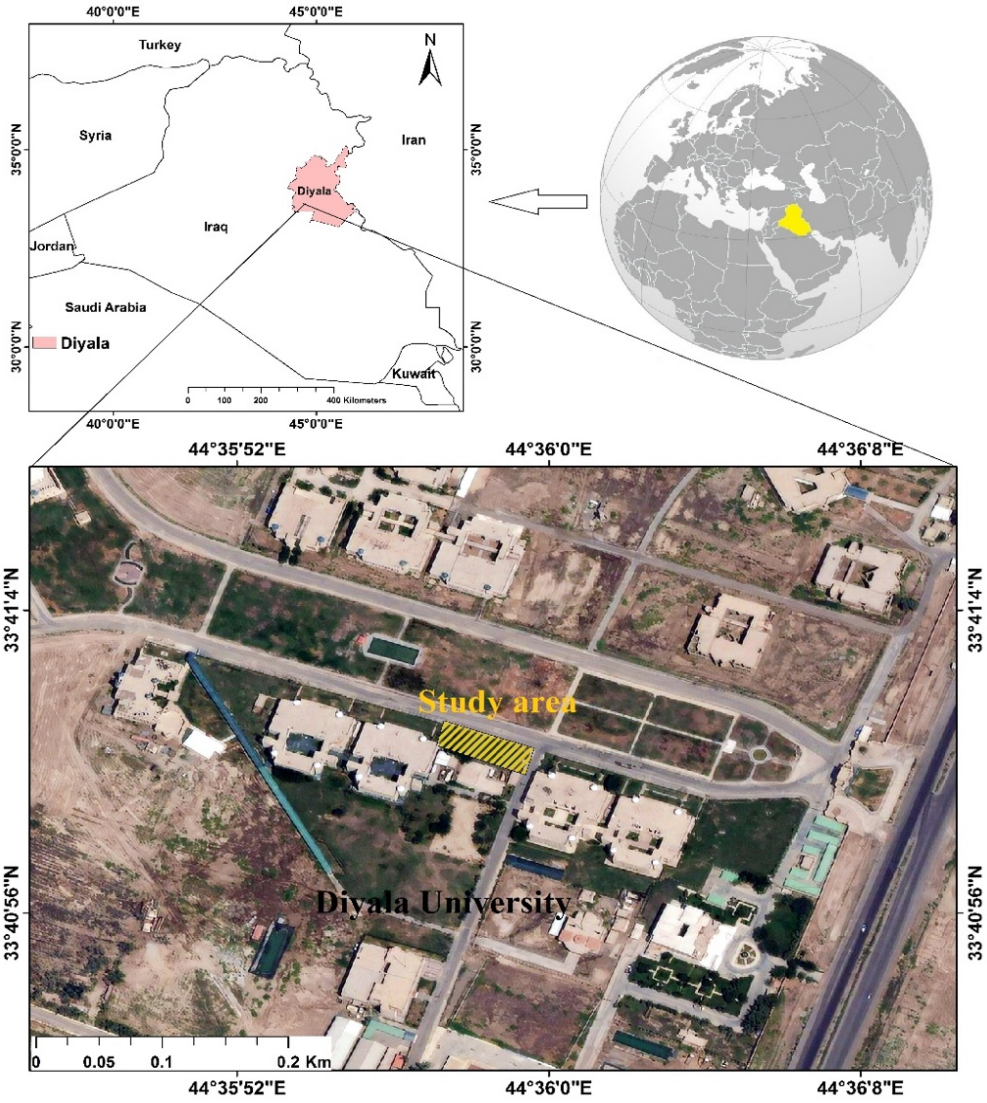

Fig. 1. The location map of the study area

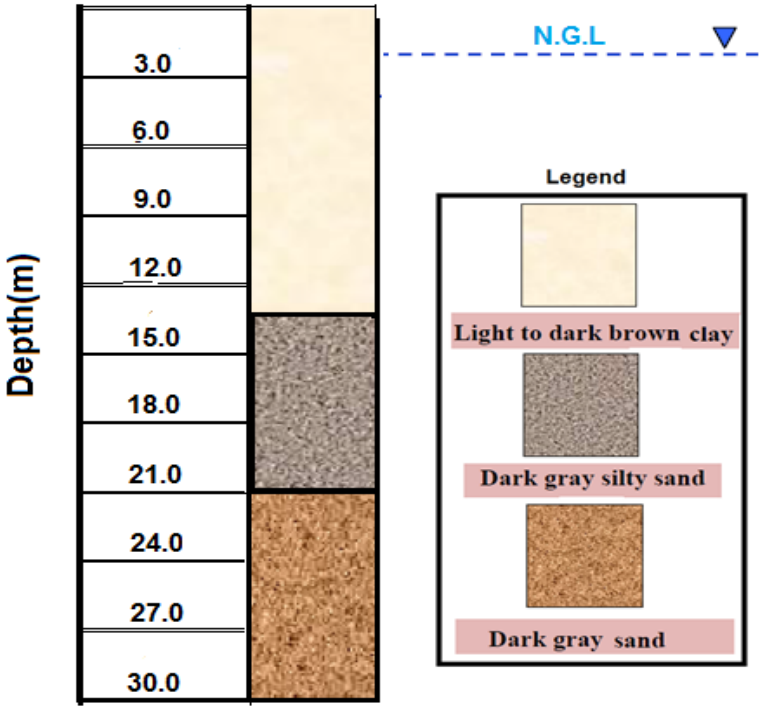

Fig. 2. The borehole section shows the soil profile and groundwater level in the study area (Al-Ebdaa Company, 2015).

3. Material & Methods

3.1 Electrical Resistivity -Basic Theory

The Electrical Resistivity Imaging (ERI) concept is based on the relation generally gives a resistance value. The primary governing Equation is Ohm's law:

$$\Delta V = R\, I \qquad (1)$$

where I is the electrical current, V is the voltage, and R is the resistance. Resistance is calculated from a known current generated by the equipment and voltage measured at the surface. Generally, the further the current travels, the greater the resistance. Besides, the less cross-sectional area the current has to travel through, the more excellent the resistance. These two properties of current flow, in conjunction with the intrinsic resistivity of the material that the current is traveling through, determine the resistance. The following Equation defines the resistance (R) as a function of the geometry of a resistor and the resistivity of the cylindrical body:

$$R = (\rho\, L) / A \qquad (2)$$

Where L is the distance traveled by the current, A is the cross-sectional area of the current path, and (ρ) is the resistivity, and by rearranging Equation (2), the resistivity can be expressed as:

$$\rho = (R\ A)/L \quad (3)$$

In this case, the apparent resistivity ρa value can be calculated by:

$$\rho a = k\ R \quad (4)$$

Where ρa is the bulk resistivity of all subsurface layers influencing the current flow **(**Milsom, 2003). From I and V, the value ρa will calculate by dividing the measured potential difference by the applied current times the geometric factor (k).

$$\rho a = k\ (V/I) \quad (5)$$

Where k is known as the geometric factor that depends on the arrangement of the four electrodes. Thus, a factor that defines the ease for I to flow through the earth is known as ρ.

3.2 Data Acquisition and Processing

3.2.1 2D ERT survey

2D ERT survey was applied in the study area using ABEM Terrameter SAS 4000 resistivity meter. Wenner-Schlumberger arrangement was chosen to carry out the measurements because of its high-resolution image, good signal strength, depth of penetration, and moderate sensitivity to vertical and horizontal structures (Loke, 2001; Abdulameer *et al*., 2018). The electrical resistivity data were collected manually along six parallel profiles covering an area of 40 x 5 m (Figure .3). For each profile, 41 electrodes with a minimum spacing of one meter were installed at the perpendicular direction to the axis of the buried sewage system. To delineate the boundaries of the septic system, additional 2D resistivity measurements were conducted along a new profile (profile 7) located between profiles 4 and 5, using a Multi-scale survey technique which described briefly by Abdul Nassir *et al*. (2000). Using this technique, the depth of penetration, resolution, and horizontal coverage of the resistivity section was increased, and hence a clear identification of the buried features was acquired (Abdul Nassir *et al*., 2000). The acquired resistivity data were inverted to resistivity sections using RES2DINV software (Loke, 2012). In the current study, the robust (blocky) optimization method was used because it gives the best results when the subsurface has sharp boundaries (Loke *et al*., 2003), as expected in the site. The model refinement option was used to take care of the large resistivity changes near the surface. With the refinement option, the program automatically reduces the unit electrode spacing it uses by half of that known in the data (Loke 2012). The 2D data files were merged into a 3D data file to perform the 3D inversion using RES3Dinv and Zondres3d software.

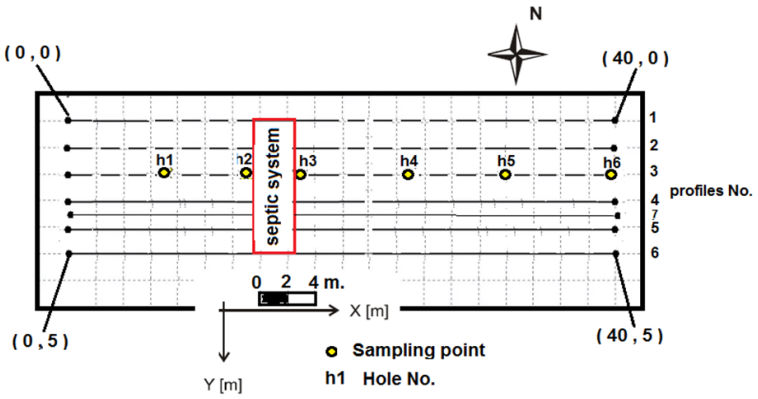

Fig. 3. The layout plan of the investigated site shows the location of resistivity profiles and soil sampling points.

3.2.2 Samples Collection and Laboratory Analysis

Six sampling holes (h1, h2, h3, h4, h5, and h6) at a depth of 1.5m along profile three were drilled during this study (figure 3). The holes (h1, h2, h3, and h4) were drilled at the site where the anomaly zones of the lower resistivity values (<1 Ω.m) were observed h2 and h3 had drilled about 0.5m away from both sides of the septic system. For the comparison, h5 and h6 were then drilled at the non-anomaly zone (relatively higher resistivity zone) 17 and 25m away from the septic system, respectively. A total of six soil samples (1 sample per hole) were collected at 1.5m depth using a hand auger. The collected soil samples were air-dried to remove moisture and sieved using sieves of <2mm size to remove coarse debris, stones, and pebbles. To increase homogeneity, the samples were grinded in a mortar with a pestle. Later soil samples were digested using the aqua regia digestion method and then analyzed for determining the concentration of Pb, Ni, Zn, Cu, and Cr by Atomic Absorption Spectrophotometry AAS (AA-7000, Shimadzu, Japan). To assess the quality of data, accuracy and precision were estimated using the formulas described by Cicchella *et al.* (2020). **Table 1** shows the accuracy and precision calculated on quality control results and detecting limits for each element. All analyses were carried out by technical staff at the laboratories of the chemistry department, Diyala University.

Table 1. Quality control results for each element

Elements	IDL (mg/kg)	Accuracy (%)	Precision (RPD %)
Pb	0.01	1.2	2.3
Ni	0.1	3.4	2.1
Zn	0.01	2.4	3.7
Cu	0.01	1.9	3.6
Cr	0.01	3.2	1.7

IDL: - Instrumental detection limit

4. Results and Discussion

4.1 ERT Data

The results of ERT surveys are displayed as resistivity – depth sections (Figures 4 and 5), horizontal depth slices (Figure 6), and three-dimensional model (Figure 7) using RES2DINV, RES3DINV, and Zondres3d software, respectively. The acquired information about the subsurface was interpreted depending on resistivity variations and their relation to the known features in the investigated site. Figure 4 shows the inverted resistivity sections for profiles 1, 2, 3, 4, 5, and 6 measured at the perpendicular direction to the axis of a covered septic system**.** Along with these profiles, the resistivity distributions can be differentiated into two main layers. The top layer has high resistivity values (> 16 Ω.m) with an average thickness of about 0.7 m. This layer can be correlated with the surface soil, consisting of fill materials. The second layer is characterized by low resistivity values (1-5 Ω.m) extending to the end of investigated depth. Based on nearby wells' information, this layer can be interpreted as a clay layer. Within this layer, a zone with relative intermediate resistivity values (6-16 Ω.m) was detected. This zone appears along all inverted sections at the study area, between holes 2 and 3 (h2 and h3). Based on available information, this zone represents the buried septic system in the study area. The buried septic system is made from concrete, and the corrosion procedure on its structure may have occurred. Therefore, it gives these resistivity values in the inverted sections due to increased moisture content in clayey soil (Neville, 2006**;** Bery *et al*., 2018**).** To delineate the boundaries of the septic system, additional 2D resistivity measurement was conducted along a new profile (profile 7) located between profiles 4 and 5, using the Multi-scale survey technique (Abdul Nassir *et al.*, 2000). The use of this technique led to increasing the depth of investigation, enhancing the information obtained from different depth levels, increasing the horizontal coverage, and thus increasing the resolution of the producing section (Abdul Nassir *et al*., 2000). Figure 5 shows the resistivity section resulting from the application of this technique along with profile 7. It can be concluded from Figures 4 and 5 that the dimension of the buried septic system can be determined. The approximate dimensions of the buried target are the height of 2m, the width of 3m, and an approximate length of 5m. Several rounded, very low resistivity anomalies (<1 Ω.m) are also shown within the clay layer, especially close to both sides of the septic system. These anomalies can be interpreted as either wetted clay layers or contaminated clay zones.

To display the 3D distribution of electrical resistivity in X Y directions with depth, horizontal depth slices were extracted (Figure 6). The first slice, which represents the resistivity distribution from the surface to 0.5 m depth, shows relatively high resistivity, reflecting the surface soil with dominant fill materials. From the second slice (after 0.5 m) to the last slice, the effect of the buried septic system appeared as relative intermediate resistivity values at the position between holes 2 and 3 (h2 and h3). Very low resistivity anomalies (< 1 Ω.m) were shown within the clay layer at depth ranges from 1.08 m to 2.5 m close to both sides of the detected septic system (slices number 3 and 4). These anomalies can be interpreted as either due to wetted clay layer or contaminated clay zones resulted from leachate migration from corroded sides of the septic system outward into

the surrounding soil. Since there is a low resistivity contrast between the clay layer and leachate, the contamination source could hardly be detected in the inverted resistivity sections. Therefore, besides the resistivity survey, the chemical analysis for soil samples was conducted to support this interpretation. Displaying the results in the form of slices helps select the most representative depth that gives a better presentation of the problem of interest. Based on the results obtained from inverted resistivity sections and horizontal depth slices (Figures. 4 and 6), the best suitable depth for collecting soil samples was chosen to be about 1.5m along with profile number 3. To get a better visualize of the selected depth in XY direction and XZ direction, Zondres3d software was used for displaying the 3D extent of the contaminated zones (Figure 7).

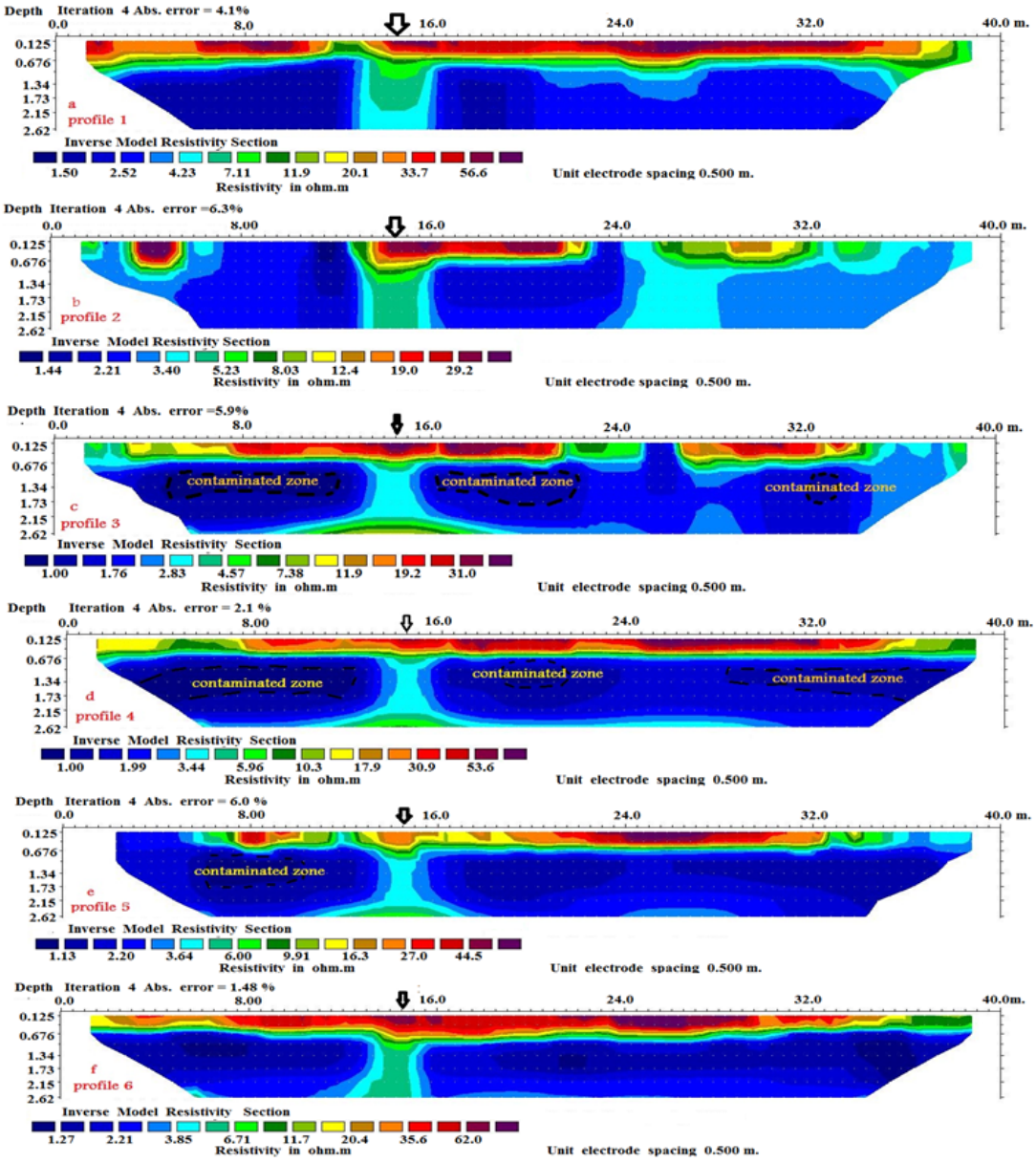

Fig. 4. Inverted resistivity sections of profiles 1, 2, 3, 4, 5 and 6

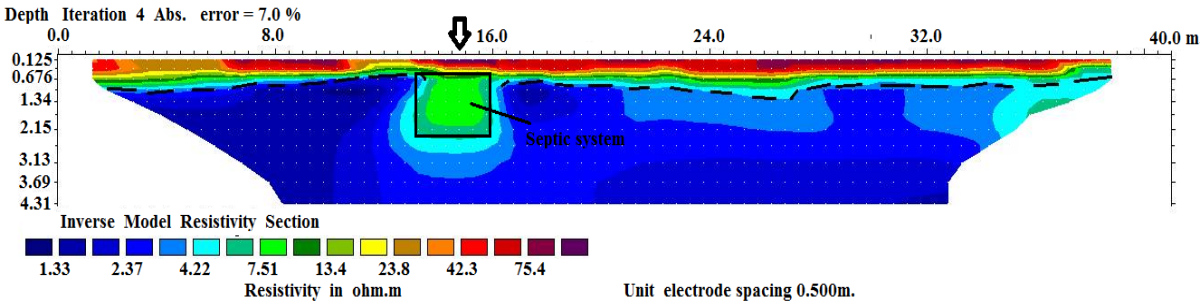

Fig. 5. Inverted resistivity section of profile 7

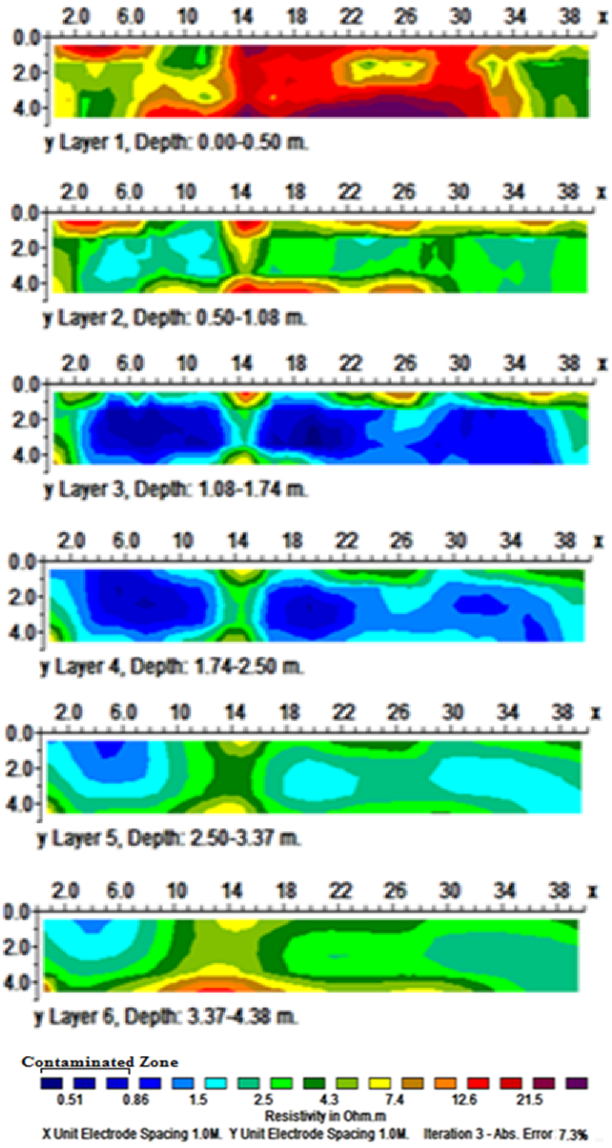

Fig. 6. Horizontal depth slices obtained from 3D ERI: the low electrical resistivity anomaly, less than (1 Ω.m) represent the contaminated zone.

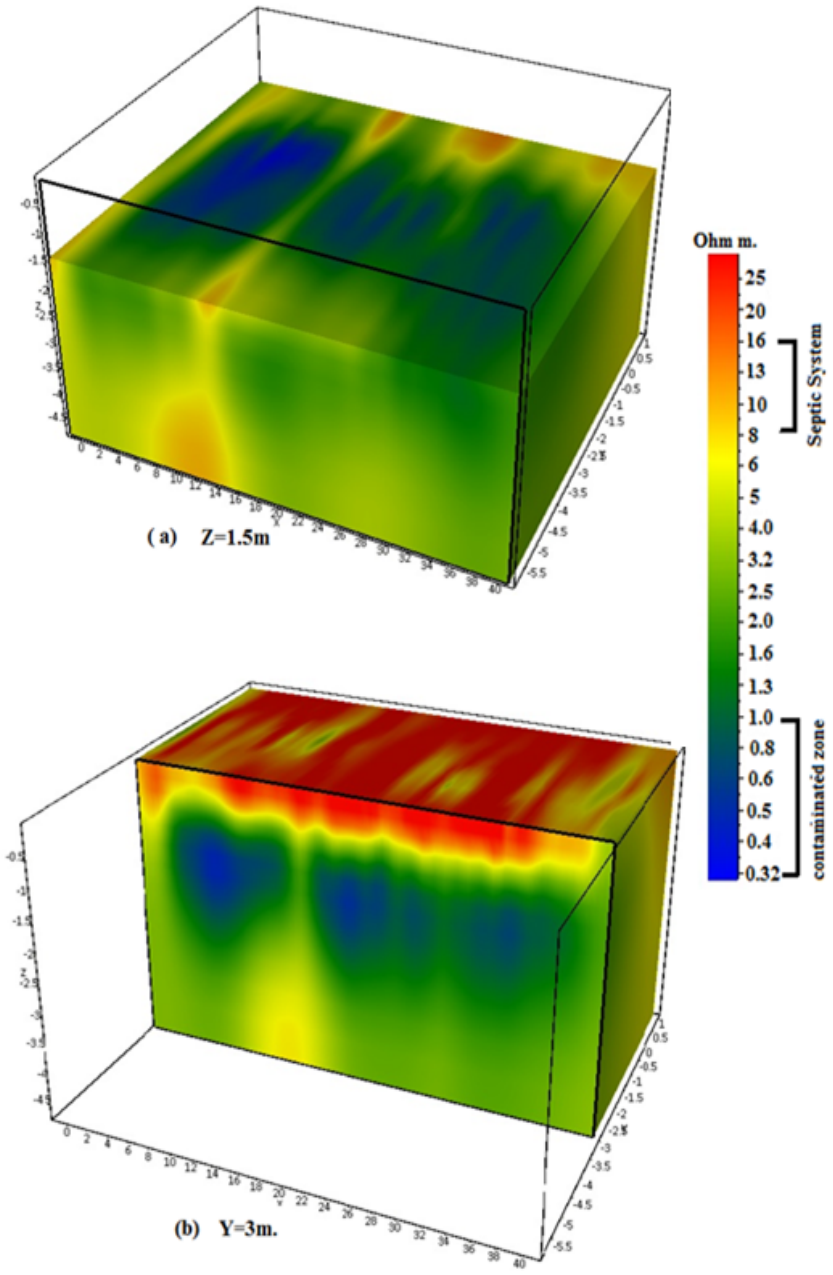

Fig. 7. Three-dimension models show the location of collected samples (a) Z =1.5 m, (b) y=3m

4.2 Soil Chemistry

The chemical analyses of the soil samples involved the determination of the concentration of lead (Pb), Nickel (Ni), Zinc (Zn), Copper (Cu), and chromium (Cr). **Table 2** shows the results of the chemical analysis, whereas the main statistical parameters for elements are shown in **Table 3**. Based on the obtained results, there was a regular decrease in the heavy metals concentration from

the septic system toward the locations away from the septic system. The histograms of the concentration levels of the analyzed metals of the sampling holes are illustrated in figure 8. The highest levels of the heavy metals concentration are observed in locations that appeared as anomaly resistivity zones (less 1 Ω.m) near the septic system, whereas the lowest levels are observed in non-anomaly resistivity zone at the location of comparison holes (h5 and h6) which drilled 17 and 25m away from septic system respectively (Figure 8 a-e).

Table 2. Heavy metal concentrations and their local background values (mg/kg)

Sampling hole No.	Pb	Ni	Zn	Cu	Cr
h1	58	61.08	89	38.20	86
h2	79.82	88.67	123	66.70	137.4
h3	85	85.44	126.9	57.60	128.79
h4	56.2	58.56	106.7	39.60	83.7
h5	43.2	50.21	89.45	35.30	81.4
h6	41.6	41.12	84.25	31.20	82.1
local natural background	51	111	99	38	133

Table 3. Statistical parameters for the heavy metal concentration of analyzed samples

Statistics

		Pb	Ni	Zn	Cu	Cr
N	Valid	6	6	6	6	6
	Missing	0	0	0	0	0
Mean		60.63	64.18	103.21	44.76	99.89
Std. Error of Mean		7.42	7.78	7.56	5.74	10.57
Median		57.10	59.82	98.07	38.90	84.85
Std. Deviation		18.19	19.07	18.52	14.06	25.90
Range		43.40	47.55	42.65	35.50	56.00
Minimum		41.60	41.12	84.25	31.20	81.40
Maximum		85.00	88.67	126.90	66.70	137.40

N: Number of samples

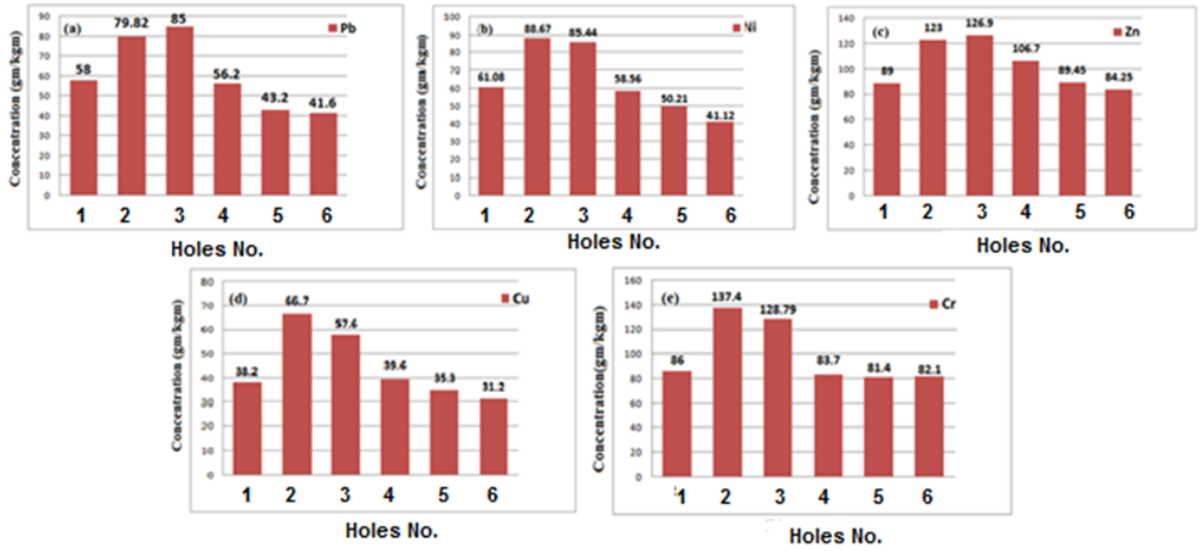

Fig. 8. Concentration levels of heavy metals in soil samples (a) Pb, (b) Ni, (c) Zn, (d) Cu, and (e) Cr.

These concentrations were also compared with the local natural background values measured in soil from rural areas close to the study site by Khwedim *et al*. (2011). The results showed that the concentrations of Pb, Zn, and Cu near both sides of the septic system (h2, h3, and h4) are higher than background values, whereas these concentrations are lower than background values at the location of other holes (h5 and h6). The concentrations of Ni and Cr at all sampling points were close or lower than the background value of the area and are not attributable to anthropogenic contamination. The increasing heavy metals concentration nearby the septic system may be resulted from leachate migration from the corroded sides of the septic system to contaminate the surrounding area and hence can be considered anthropogenic. The leachate migration is not widely spread laterally or vertically due to the low porosity of clayey soil. Therefore, low concentrations of heavy metals were observed at the locations away from the septic system, indicating that these locations were unaffected by leachate migration. Although the investigated system is a household kind and small size, its age and cumulative effect compensate for the size. The geophysical survey and soil analysis results show that the environment is impacted by the sewage system.

5. Conclusion

The results of the ERT survey showed that the study objectives were successfully achieved. The geoelectrical imaging technique has been effective in detecting the buried septic system and mapping its environmental impact within the University of Diyala Campus in northeastern Iraq. The buried septic system appeared as a relatively intermediate resistivity zone with 3m width and at 0.7 m depth along with all profiles at the study site. The prior known information corroborative this location. The survey results also yielded very low resistivity zones at locations close to the septic system, which are likely to be the impacted areas. These results correlated with the concentrations of heavy metals measured for the soil samples. The concentrations of Pb, Ni, Zn,

Cu, and Cr in soil samples obtained close to the septic tank were higher than that obtained at locations away from the septic tank. Except for Cr and Ni, which showed values close to the background level, the Pb concentration, Zn, and Cu were also higher than the local background level of the area. The high concentrations of heavy metals and very low resistivity values close to the septic tank support the evidence of leachate migration from the corroded sides of the sewage system into the surrounding soil. The results demonstrate that the method presented in this study holds promise as a tool for mapping contaminated soil in an urban environment. It is also recommended that the electrical resistivity tomography survey should be made before sampling soil to locate the best site for collecting soil samples.

References

Abdul Nassir, S.S., Loke, M.H., Lee, C.Y., & Nawawi, M.N. (2000) Salt-water intrusion mapping by geoelectrical imaging surveys. Geophysical Prospecting, 48 (**4**): 647-661.

Abdulameer, A., Thabit, J.M., AL-Menshed, F.H., & Merkel, B. (2018) Investigation of seawater intrusion in the Dibdibba Aquifer using 2D resistivity imaging in the area between Al-Zubair and Umm Qasr, southern Iraq. Environmental Earth Sciences, **77**(**17**): 619.

Abdulrazzaq, Z.T., Al-Ansari, N., Aziz, N.A., Agbasi, O.E., & Etuk, S.E. (2020) Estimation of main aquifer parameters using geoelectric measurements to select the suitable wells locations in Bahr Al-Najaf depression, Iraq. Groundwater for Sustainable Development, 11, 100437.

Abed, A. M., Al-Zubedi, A.S., & Abdulrazzaq, Z.T. (2020) Detected of gypsum soil layer by using 2D and 3D electrical resistivity imaging techniques in University of Anbar, Iraq. Iraqi Geological Journal, 53(**2C**): 134-144.

Aizebeokhai, A.P. (2009) Geoelectrical Resistivity Imaging in Environmental Studies. In: Yanful, E.K. (Ed.) Appropriate Technologies for Environmental Protection in the Developing World. Pp. 297-305. Springer, Dordrecht.

Al-Ebdaa Company (2015) Soil investigation report for the new buildings of Diyala university_ part11, Report No.: ESR-015-08, Pp. 210.

Amidu, S.A. & Olayinka, A.I. (2006) Environmental assessment of sewage disposal systems using 2D Electrical-Resistivity Imaging and geochemical analysis: A Case study from Ibadan Southwestern Nigeria. Environmental and Engineering Geoscience, **7**(**3**): 261–272.

Aziz, N.A., Abdulrazzaq, Z.T., & Agbasi, O.E. (2019) Mapping of subsurface contamination zone using 3D electrical resistivity imaging in Hilla city, Iraq. Environmental Earth Science, 78 (**16**): 502.

Bery, A.A., Nordiana, M.M., Ismail, N.E. H., Jinmin, M., & Amalina, M.N. (2018) Buried Man- made Structure Imaging using 2-D Resistivity Inversion. Journal of Physics, Conference Series, 995(1): 012075**.**

Chik, Z., Murad, O.F., & Islam, T. (2014) Geo-Environmental Characterizations in Heavy Metal and Oil Contaminated Soil Using Soil Electrical Resistivity. Advances in Environmental Biology, 8(**22**): 138-146.

Cicchella D., Zuzolo D., Albanese S., Fedele L., Di Tota I., *et al.* (2020) Urban soil contamination in Salerno (Italy): Concentrations and patterns of major, minor, trace and ultra-trace elements in soils. Journal of Geochemical Exploration, 213: 106519.

Dahlin, T. (2001) The development of DC resistivity imaging techniques. Computers and Geosciences, 27(**9**): 1019–1029.

Gemail, K.S., Attwa, M., Eleraki, M., & Zamzam, S. (2017) Imaging of wastewater percolation in heterogeneous soil using electrical resistivity tomography (ERT): a case study at the east of Tenth of Ramadan City, Egypt. Environmental Earth Science, 76(**19**): 666.

Giang, N.V., Kochanek, K., Vu, N.T. & Duan, N.B. (2018) Landfill leachate assessment by hydrological and geophysical data: case study NamSon, Hanoi, Vietnam. Journal of Material Cycles and Waste Management, 20(**3**):1648-1662.

Granato, G. E. & Smith, K.P. (1999) An automated process for monitoring groundwater quality using established sampling protocols. Ground Water Monitoring and Remediation, 19(**4**): 81-89.

Hamed, M., Ali K., Mohammad B., Fatollah G., Borujeni , *et al.* (2017) Industrial waste characterization and management in Arasanj industrial estate, Iran. Kuwait journal of science, 44(**3**):104-111.

Hamzah, U., Jeeva, M., & Ali, N.M. (2014) Electrical Resistivity Techniques and Chemical Analysis in the Study of Leachate Migration at Sungai Sedu Landfill. Asian Journal of Applied Sciences, **7**(**7**): 518-535.

Jassim, Z., & Goff, J.C. (2006) Geology of Iraq. Published by Dolin, Prague and Moravian Museum, Brno, Pp.341.

Kabata-Pendias, A. (2010) Trace elements in soils and plants. 4th edition, CRC Press, Boka Raton, Pp.548.

Kareem K.H., Hussein, S.A., & Al-Adely J.A. (2011) Heavy Metals in some soils of Baquba city: determination, Distribution and Controlling Factors. Diyala journal of pure sciences, **7**(**2**):166-183**.**

Liu, H., Yang, H., & Yi, F. (2016) Experimental study of the complex resistivity and dielectric constant of chrome contaminated soil: Journal of Applied Geophysics, 13(**1**): 109–116.

Loke, M.H. (2001) Electrical Imaging Surveys for Environmental and Engineering Studies. A Practical Guide to 2-D and 3-D Surveys. RES2DINV Manual. IRIS Instruments.

Loke, M.H. (2012) Tutorial 2-D and 3-D electrical imaging Surveys. Pp.172

Loke, M.H., Acworth, I., & Dahlin, T. (2003) A comparison of smooth and blocky inversion methods in 2D electrical imaging surveys. Exploration Geophysics 34(**1**): 182–187.

Metwaly, M. & Fouzan, A., (2013) Application of 2-D geoelectrical resistivity tomography for subsurface cavity detection in the eastern part of Saudi Arabia. Geoscience Frontiers, 4**(4)**: 469-476.

Milsom, J. (2003) Field Geophysics, 3rd Edition, John Wiley and Sons Ltd.

Nasir, U., Khan, M.J., Imran, M., Khan, M.R., Farooq, M. *et al*. (2021) Groundwater investigations in the Hattar industrial estate and its vicinity, Haripur district, Pakistan: An integrated approach. Kuwait Journal of Science, 48 (**1**): 51- 61.

Neville, A. M. (2006) Properties of concrete, 4th ed., Pearson Prentice Hall, Edinburgh Gate, England. Pp. 321.

Olaseeni, O.G., Sanuade, O.A., Adebayo, S.S. & Oladapo, M.I. (2018) Integrated geoelectric and hydrochemical assessment of Ilokun dumpsite, Ado Ekiti, in southwestern Nigeria. Kuwait Journal of Science, 45(**4**): 82-92.

Porsani, J.I., Elis, V.R., Shimeles, J.C. & Moura, H.P. (2004) The use of GPR and VES in delineating a contamination plume in a landfill site: a case study in SE Brazil. Journal of Applied Geophysics, **55**:199-209.

Rao, G.T., Rao, V.V., Padalu, G., Dhakate, R. & Sarma, S.V (2014) Application of electrical resistivity tomography methods for delineation of groundwater contamination and potential zones. Arabian Journal of Geosciences, **7**:1373–1384.

Rizzo, E. & Valeria ,G. (2019) New deep electrical resistivity tomography in the High Agri Valley basin (Basilicata, Southern Italy), Geomatics, Natural Hazards and Risk, 10(**1**):197-218.

Thabit, J.M. & Khalid, F.H. (2016) Resistivity imaging survey to delineate subsurface seepage of hydrocarbon contaminated water at Karbala Governorate. Iraq. Environmental Earth Science, 75**(1)**:87.

Wang, Y., Ya Xu, Changxin N., & Lu Don (2019) Assessment of Chromium Waste Contamination by Electrical Resistivity Tomography: A Case Study. Journal of Environmental and Engineering Geophysics. 24(**1**):163 -167**.**

Submitted: 03/10/2020
Revised: 25/03/2021
Accepted: 04/04/2021
DOI: 10.48129/kjs.10674